Transonic High Reynolds Number Transition Experiments in the ETW Cryogenic Wind Tunnel

Jean Perraud[1] and Jean-Pierre Archambaud[2]
ONERA Toulouse, 31055 France

Geza Schrauf[3]
Airbus, D-28199 Bremen, Germany

Raffaele Donelli[4]
CIRA – Italian Aerospace Research Center, Capua, 81043 Italy

Ardeshir Hanifi[5],
FOI – Swedish Aerospace Research Center, SE-164 90, Stockholm, Sweden

Jurgen Quest[6],
European Transonic Windtunnel, D-51147, Cologne, Germany

Thomas Streit[7],
DLR, German Aerospace Center, D-38108 Braunschweig, Germany

and

Stefan Hein[8], Uwe Fey[9], Yasuhiro Egami[10],
DLR, German Aerospace Center, D-37073 Göttingen, Germany

With the goal of studying Natural Laminar Flow (NLF) wings for future 'green' transport aircraft, the aim of the European Research Project TELFONA is to develop and demonstrate the possibility of testing full aircraft models with NLF wings at large Reynolds numbers in the cryogenic Wind Tunnel ETW. Two main steps were defined, first the design and test of a 'calibration' model, to be followed by a realistic transport aircraft model. This paper is dedicated to the first one, which was especially designed in order to allow a calibration of the Wind Tunnel transition N-factors at large values of the chord Reynolds number typical of testing in ETW. The paper will describe these different phases of the activities, from design, testing and numerical validation, with a focus on the validation and calibration of transition prediction tools. Examples of numerical results obtained by the project partners will be confronted to the experiments.

[1] Research Engineer, Models for Aerodynamics and Energetics Depart., AIAA member, jean.perraud@onera.fr
[2] Research Engineer, Models for Aerodynamics and Energetics Depart., jean-pierre.archambaud@onera.fr.
[3] Senior Research Scientist, Senior Member AIAA, geza.schrauf@airbus.com.
[4] Research Engineer, Applied Aerodynamics Lab, r.donelli@cira.it
[5] Director of Research, Div. of Defence & Security, Systems and Technology, ardeshir.hanifi@foi.se
[6] Chief Aerodynamicist, Associate Fellow AIAA, jq@etw.de
[7] Research Engineer, Inst. of Aerodynamics and Flow Technology, th.streit@dlr.de
[8] Research Scientist, Inst. of Aerodynamics and Flow Technology, stefan.hein@dlr.de
[9] Research Scientist, Inst. of Aerodynamics and Flow Technology, uwe.fey@dlr.de
[10] Research Scientist, formerly DLR, now at Nagoya University, Nagoya, Japan, y.egami@coe.mech.nagoya-u.ac.jp

Nomenclature

C_p = pressure coefficient
C_L = Lift coefficient
c = chord
k = total wavenumber (m^{-1}) $k^2 = \alpha^2 + \beta^2$
β^* = dimensional spanwise wavenumber $\beta^* = \beta/\delta_1$
ψ = direction of the wave vector with respect to the external velocity
φ = sweep angle

I. Introduction

The objective of a fifty percent reduction in aircraft fuel consumption, (together with eighty percent reduction in nitrogen oxides and 6 dB in perceived noise level), was introduced in 2001 by the European Union in the 'Vision 2020' for European Aeronautics, and requires breakthrough achievements related to drag reduction and propulsion efficiency. Similar trends may be expected in the USA. Laminar flow technology may be seen as a promising candidate to contribute to this objective, as the extended laminar flow region allows a strong decrease in friction drag. Laminar flow may be attained by shape modification (Natural Laminar Flow, NLF), possibly associated with wall suction (Hybrid Laminar Flow Control, HLFC). Another line of research dealing with 'long endurance UAVs' also calls for a large reduction of total drag, including friction drag.

In the past, a number of flight demonstrators were successfully used both in the USA[1,2] and in Europe (Falcon 50[3] and 900, ATTAS, Fokker 100[4], Airbus A320[5]). Flight tests were selected as they allow full system demonstration at flight Reynolds numbers which are not attainable in conventional wind tunnels: maximum chord Reynolds number Re_C in a transition test in transonic flow in the ONERA S1Ma facility is about 15×10^6. On the other hand, such flight tests are much too expensive to allow for extensive parametric exploration and optimization.

As the ETW cryogenic wind tunnel allows chord Reynolds numbers up to $Re_C = 30\times10^6$ by combining cryogenic temperatures (down to 115 K) and pressurization (up to 3 bar), the TELFONA European Research Project, led by Airbus, was launched to demonstrate the use of ETW for NLF wing design at large Reynolds numbers. Two main steps were defined, first the design and test of a 'calibration' model, to be followed by a more realistic transport aircraft model. This paper is dedicated to the first of these two models, called 'Pathfinder', which was especially designed in order to allow the calibration of the Wind Tunnel transition N-factors, in the frame of the e^N method[6,7], at large values of chord Reynolds number typical of testing in ETW. Figure 1 shows the ranges in Reynolds number versus sweep angles of various wind tunnels and flight tests, with the corresponding expected domain for the Pathfinder experiment.

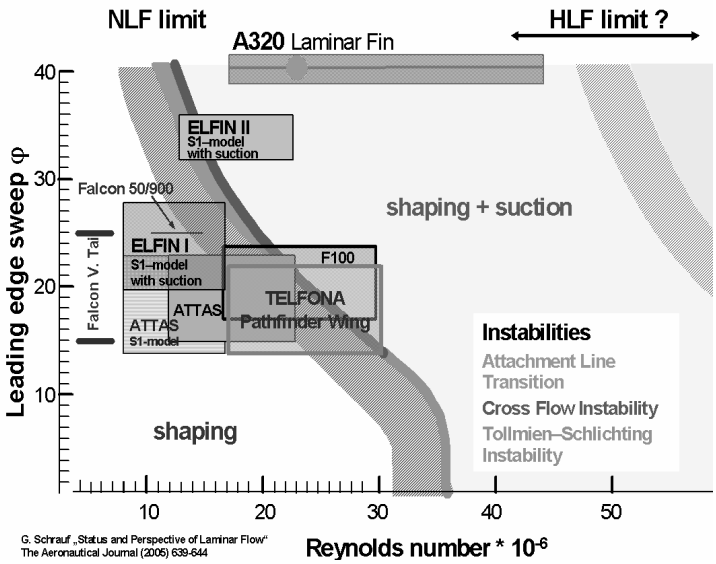

Figure 1. Various wind tunnel and Flight Laminar wing experiments in a Reynolds number versus Sweep angle domain.

The first part of the paper will deal with model design and specific instrumentation for transition detection in cryogenic conditions. Then typical experimental results will be presented, followed by stability analysis and N-factor correlations for this model in ETW. Stability analysis was applied after the tests in order to 'calibrate' the various tools currently used by research labs in Europe, including simplified database, local linear and non-local linear stability approaches. Examples of numerical results obtained by the project partners will be compared to the experiments.

II. Model Design

The full span Pathfinder model was designed by CIRA, DLR, Airbus and ONERA for the calibration of transition measurements in ETW. A simple swept planform with a low taper and 18 deg. sweep angle was selected. This leading edge sweep was chosen knowing that additional side slip would allow the examination of the effect of sweep angle variation on leading edge crossflow transition. The wing section was then determined such that the N-factor evolution coming out of stability calculation would grow linearly over the longest possible chordwise distance. In a first step, candidate aerofoil sections were designed independently by the three partners, each using their preferred design toolsets. CIRA used a boundary layer coupled Euler method with an ONERA transition prediction method. DLR used an inverse design procedure based on the FLOWer code, whilst ONERA preferred to modify the existing Fokker 100 glove aerofoil using the elsA code. The three proposed aerofoils were then reviewed, and the DLR LV5 aerofoil was selected. This LV5 aerofoil was derived from an ATTAS laminar glove section and modified for the higher Mach number (M=0.78) flow condition. In the following phase, the final wing design was conducted in the presence of a prescribed fuselage geometry with belly fairing from an existing ETW model. The DLR inverse design method[8] for transonic wings was applied in order to obtain parallel isobars from 30 to 70 % of span for the design point M=0.78, Re=20×10^6, C_L = 0.216, as shown in Fig. 2. While at the design point the designed wing has a constant pressure distribution in the region of interest, analysis performed at off-design points showed that the spanwise variation of sectional pressure distributions is sufficiently weak. Therefore for the Pathfinder wing, stability analysis based on either numerical or experimental data can be attributed to a pressure distribution from a constant span section. Finally, Airbus analyzed the pressure distributions supplied by DLR for design and off-design conditions using linear stability theory in the LILO code[9]. A typical result is shown in Fig. 3, where the N-factor based on incompressible constant wavevector direction ψ is used to evaluate Tollmien Schlichting (TS) growth, and an N-factor based on incompressible constant spanwise wavenumber β^*, at zero frequency, are used to evaluate the growth of crossflow (CF)modes.

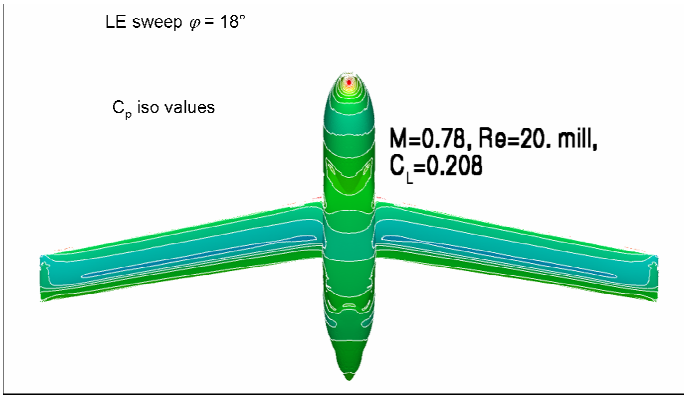

Figure 2. View of the model with pressure distributions.

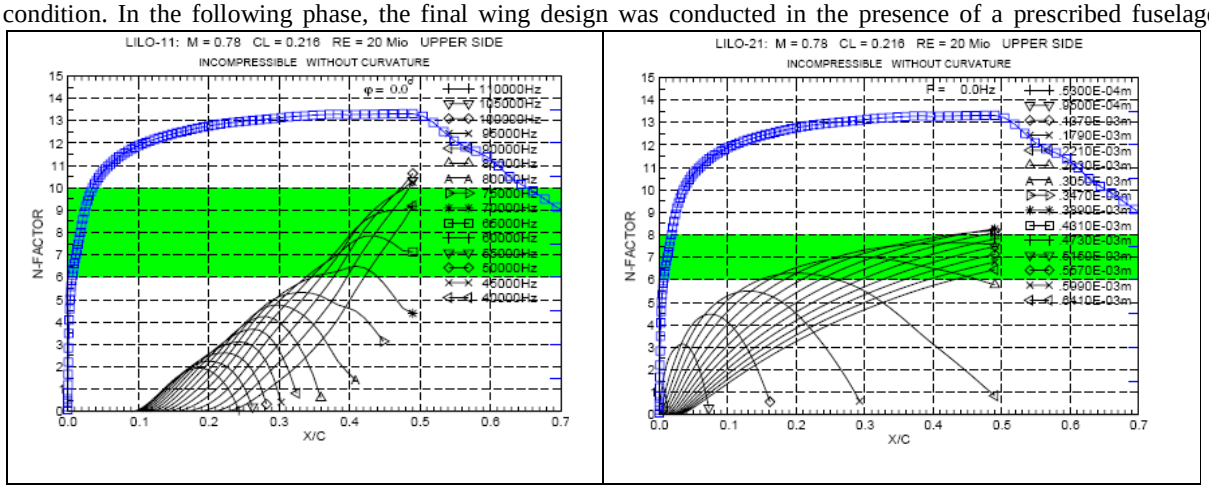

Figure 3. Pre-test stability computation for design conditions.

Mach number	Lift coefficient	Sweep angle	Re_C (Millions)	TS	CF	Mixed
0.78	0.11	18°	20	1	1	
0.78	0.22	18°	20		1	1
0.78	0.33	18°	20		1	1
0.76	0.22	18°	20			1
0.80	0.22	18°	20		1	
0.78	0.11	14°	20	1		1
0.78	0.11	22°	20	1	1	
0.78	0.22	22°	20		2	
0.78	0.33	22°	20		2	
0.76	0.11	14°	20	1		
0.76	0.11	18°	20	2		
0.76	0.33	22°	20			1

Table 1. List of cases selected at the end of pre-test computations

Figure 4. View of the model with 2 patches of TSP on the upper side

III. Pre-Tests Stability Computations

Based on computed pressure distribution, a first numerical simulation of the experiments was conducted based on the final model geometry. The range of conditions covered by the wind tunnel was explored, resulting in typical N-factor curves as shown in Fig. 3. The isolated curve shows the pressure distribution, while the grouped curves are obtained on the left side with the constant ψ strategy for incompressible flow for frequencies between 11 and 40 kHz, and on the right side with the constant β^* strategy for stationary modes. These N-factor curves contribute to an envelope, visible on the figure, which is indeed almost linear with x/c distance, as required. These pre-test computations indicated that more crossflow situations were to be expected, re-enforcing the interest for non zero side slip angle situations for generating TS cases. From the N-factor survey of the Pathfinder model performed in this pre-test stability analysis[10] twenty one flow conditions, given in table 1, were identified with interesting stability behavior for calibrating ETW. As indicated in the table, there are six TS, nine CF and five mixed cases with strong TS and CF amplification.

IV. Measurement systems for cryogenic transition detection

Two lines of pressure taps were installed on each wing, as well as patches, applied on both suction and pressure sides, of a two component cryogenic temperature-sensitive paint (cryoTSP). This paint[11] is composed of two kinds of luminescing molecules incorporated into a transparent binder. These molecules re-emit light with an intensity depending on temperature when excited by incident light in a given wavelength range. First, a "standard" molecule (Ruthenium-complex Ru) is used, which works in the range 100 K < T < 240 K. Best operating temperature for this molecule is around 180 K, because it then exhibits the best relation of sensitivity and brightness. The sensitivity for Ru decreases for T > 240 K, but with rapidly increasing signal to noise ratio (S/N) because of the much lower intensity. Highest sensitivity for the Ruthenium is around 240 K, but with 20 times less intensity compared to 160 K, for example, making exposure times extremely long (despite the high signal to noise ratio). In order to improve the cryoTSP response for the "warm" temperatures (240 K < T < ambient), DLR (Y. Egami) included a second molecule (Europium complex) into the original paint (developed by Jaxa), in addition to the Ruthenium. This Europium complex shows good sensitivity and high brightness for the warmer temperatures, where the Ruthenium complex becomes less suited. The selection of one or other molecule is determined by the wavelength of the incident light. A Xenon UV-flashlight excites the Europium and not the Ruthenium. Therefore UV light, and Europium, is used in the range 240 K < T < ambient. When performing transition detection at cold temperatures, the Ruthenium molecule is selected by changing the excitation light from UV to blue range (around 455nm), using light emitting diode (LED) illumination. Europium, on the other hand, is not excitable by the LEDs.

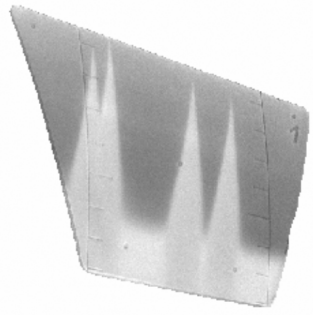

Figure 5. Example of transition detection at a low Reynolds number of 7 M.

The molecules then emit red light with temperature-dependent intensity, which is recorded by a number of CCD cameras. The wall temperature difference between laminar and turbulent boundary layer can thus be detected by the cryoTSP method, allowing the visualization of the boundary layer transition. On the pathfinder model, shown in Fig. 4, very thin, custom-built pockets on the wing's upper and lower surfaces have been sprayed with the TSP and polished to a very smooth surface, in-line with the metallic surface adjacent to the TSP areas. These four patches may be identified using the number visible on one corner (see Fig. 5): 1 and 2 for the upper side, 3 and 4 for the lower side, 1 and 3 corresponding to the right wing.

In order to increase spatial variations of temperature on the model wall, linked to the boundary layer nature, a thermal imbalance is required. This is obtained by changing the flow temperature in a stepwise manner, by about ten degrees. Following this change, a number of TSP images are recorded. Pressure measurements are realized before and after the TSP recording, in order to detect accidental changes during the test. An example of temperature visualization at 7 million Reynolds number is shown in Fig. 5, with the flow coming from the top. The image on Fig. 5 is a raw image with laminar region in grey and turbulent ones in white. Reversed contrast is used on fully processed images shown in the rest of the paper.

V. Wind Tunnel Tests

Three short experimental test campaigns were realized with the Pathfinder model, each improving the handling of the wind tunnel, the model and its instrumentation for these difficult measurements. Unusual precautions proved necessary in order to reduce to a minimum the presence of small particles in the flow, those particles causing turbulent wedges when impacting near the attachment line of the wing. Enquiry into the nature of these particles proved that there was no humidity, i.e. no ice particles in the nitrogen flow. This allowed very low temperatures, of

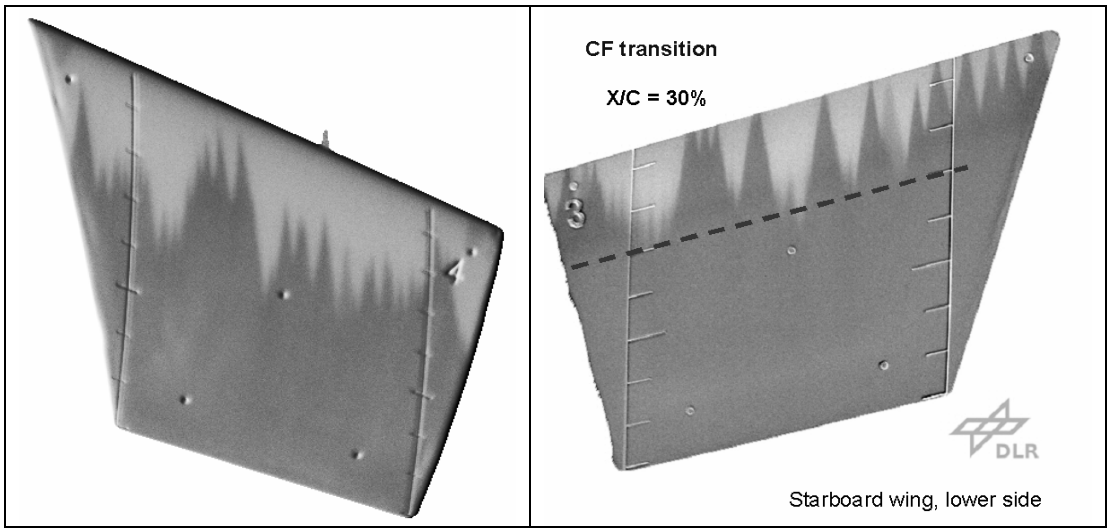

Figure 6. Typical TSP images at Re_C = 10 (left) and 20 (right) millions.

about 115 K, to be used. Typical results for the lower side are shown on Fig. 6 at chord Reynolds numbers of 10 and 20 million. The right image, showing crossflow transition, was obtained at Mach 0.78 with a static temperature of 156 K and with a side slip angle of 4 deg. The left image, also CF, was obtained at the same Mach number, a temperature of 175 K, and a larger static pressure close to 3 bar. In the course of these experiments, the Reynolds number range 7 to 23×10^6 was explored. It was observed that below Reynolds number 15×10^6 transition would in general be imposed either by the shock, on the upper side, or by the pressure recompression on the lower side. In those cases, the experiment would not provide interesting results with regard to the calibration of the N-factor methods. The most interesting results were obtained at 20×10^6 and are summarized in table 2.

The four cases selected for further analysis are highlighted in the table. As a concluding remark, it should be noted that although this experiment was difficult ETW produced a very large amount of results in a very short timeframe.

Test number, Cp	Test number, TSP	Mach	ReC (millions)	T (K)	CL
P079	P080	0.78	20	175	0
P081	P085	0.78	20	175	0.1
P086	P087	0.78	20	175	0.21
P088	P089	0.78	20	175	0.32
P090	P091	0.78	20	175	0.4
P092	P093	0.78	20	175	0.5

Table 2. Cases selected for stability analysis

VI. Analysis of results

Raw measurements obtained after the experiments required some post treatment before further analysis. Raw TSP images may be improved by averaging and numerical treatments. Figure 5 shows an example of raw data obtained at Reynolds number 7×10^6. The images on Fig. 6 are typical of the final stage of treatment. On such small models, the number of pressure taps is always kept to a minimum because of space constraints. Careful treatment of the pressure distribution is always necessary, and was conducted in this case by Airbus[12], who determined the location of the attachment line and the effective sweep, and produced sets of interpolated pressure coefficients C_p in formats adapted for boundary layer computation, as illustrated in Fig. 7. Airbus also performed boundary layer calculations and provided boundary layer data to the other partners involved.

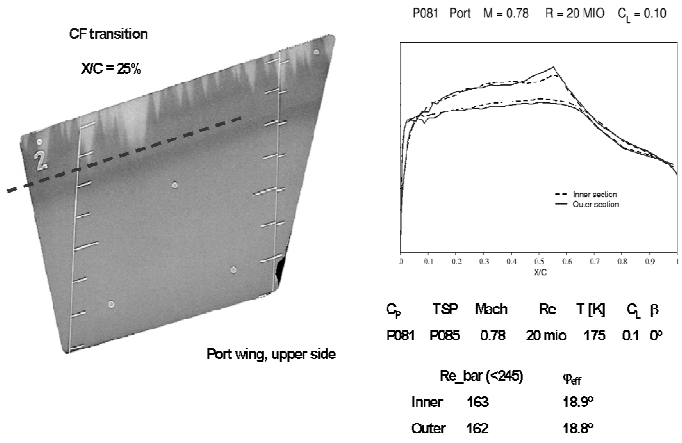

Figure 7. Typical dataset for analysis of experimental results.

A. Local Stability Theory

Although more sophisticated approaches are now available for computing the growth of instabilities in boundary layer flows, local theory remains a relevant engineering tool for two reasons: (1)-scatter of transition N-factors from flight experiments showed no statistical improvement when comparing local theory with linear PSE, and (2)-local stability calculation can be made fast and robust enough as to become a component in industrial CFD tool. Presently, it is accepted that non-local stability allows a better evaluation of the physics controlling instabilities, and that non-linear stability is a powerful tool when dealing with complex issues like flow control.

When dealing with the e^N transition prediction approach applied to the local stability of 3D flows, there exist a number of methods based on different N-factor integration strategies. Airbus (G. Schrauf) advocates for the so-called N_{TS}/N_{CF} method, in which N_{TS} is obtained by using the constant ψ strategy at frequencies covering the complete range of unstable waves, and N_{CF} is obtained by considering only stationary instabilies, using either the constant wavelength strategy or the constant spanwise wavenumber β^* strategy. In this approach, the N-factors are computed considering only incompressible equations, even though the cases of interest are transonic. A robust and efficient code, LILO, has been developed based on this method, and is integrated into a compressible boundary layer code. Another strategy commonly used is the envelope method, in which the amplification rate belonging to the most unstable solution is selected and integrated to form an N-factor curve. Results of local stability theory from ONERA, DLR, Airbus, and CIRA are presented in Fig. 8, based on the N_{CF}/N_{TS} and the envelope methods. ONERA used the in-house code CASTET[13], DLR and Airbus used LILO[9], and CIRA an improved version of COSAL[14]. Results in Fig. 8, with TS cases to the right and CF cases to the left, show the typical crossing of N_{TS} and N_{CF} curves between the two types of transition. On the other hand, the envelope method produces a quite large dispersion of results and cannot be considered well adapted for this type of situation.

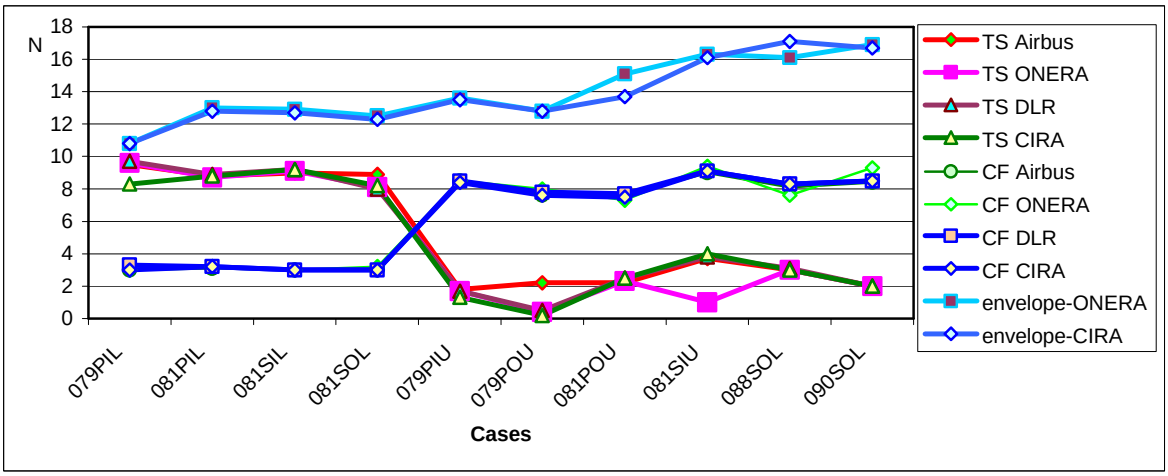

Figure 8. Local stability results obtained with two strategies: incompressible NCF/NTS and compressible envelope method

B. The Database Method

A number of models have been created at ONERA to allow rapid estimation of the amplification rates corresponding to local theory[15]. This database method allows the definition of longitudinal and crossflow N-factors similar to what is done in the N_{TS}/N_{CF} strategy, as well as an estimation of the envelope N-factor. In this case again, the method is robust and fast, and is integrated into a boundary layer code for transition prediction. Numerical results are shown in Fig. 9, compared to the equivalent local stability results. Two main differences in the definitions of N-factors have here a visible effect. First, the database is applicable to compressible flows, which explains the difference in N_{TS} values for TS cases. Second, database N_{CF} are defined using an envelope method at zero frequency, instead of a constant spanwise wavenumber strategy, which explains the vertical shift between the two curves. Nevertheless, a similar crossover is observed as in the previous figure, and the N_{CF}/N_{TS} based on the database method can also be used for transition prediction, at a fraction of the computing time necessary for any exact method.

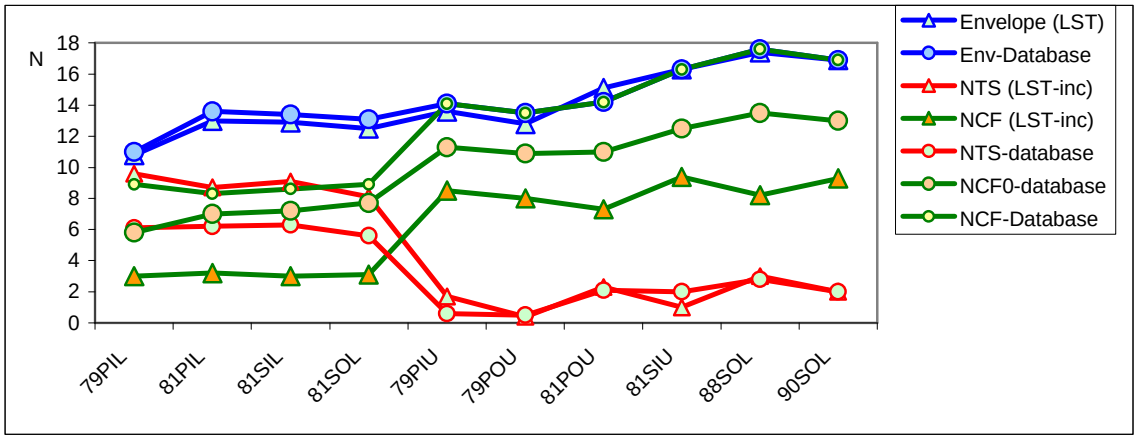

Figure 9. Comparing Local stability results with ONERA Database results.

C. Non-Local Stability Theories

Local theories do not take into account the rate of change of the mean flow. As curvature terms are of same order as non-local terms, they should also be excluded. Non-local theories, either Parabolized Stability Equations (PSE) or the multiple scale approach, include the missing terms. PSE codes from FOI and DLR (the NOLOT code[16,17]), and a code based on the multiple scale approach from CIRA (the NOLLI code[18]) were also used to analyze the Pathfinder data.

All these methods assume no variations of the mean flow in the spanwise direction, and are well adapted to consider swept wings. As in local theory the N_{CF} values are obtained by considering only stationary disturbances by imposing f=0 Hz. However, there is no equivalent integration strategy as for N_{TS} in local theory. The envelope of envelope method, more time consuming, requires N-factor computations for all unstable spanwise wavenumbers and frequencies.

Examples of results are presented in Fig. 10, obtained with two different formulations. An excellent agreement is observed between CIRA, with the NOLLI code, and DLR and FOI using two versions of NOLOT. The results obtained here show that a distinct value of transition N-factor must be used when dealing with TS or with CF cases. A zero frequency N-factor would allow to identify CF and TS cases, so that N-factor method may also be effectively used based on non-local computations.

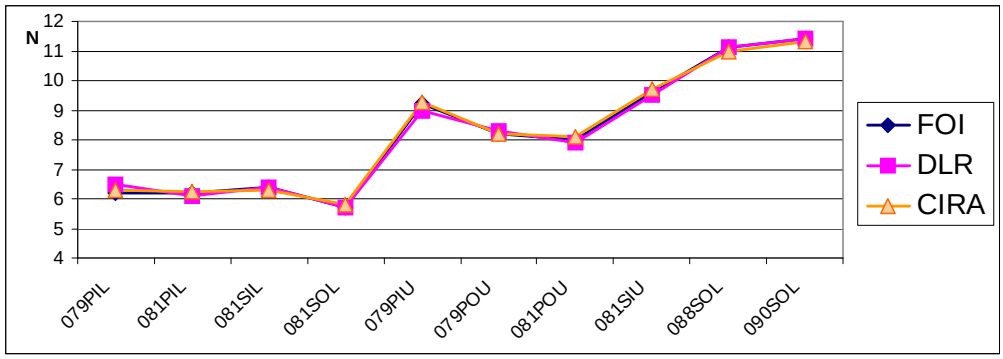

Figure 10. Non-local stability results (compressible with curvature).

VII. Conclusion

Careful design of the Pathfinder model was conducted in order to allow the calibration of ETW in a large range of Reynolds numbers. The goal of this calibration is to determine transition N-factors for both crossflow (CF) and longitudinal (TS) instabilities, knowing that TS N-factors are mostly related to non-stationary disturbances caused e.g. by free-stream turbulence or noise, while CF N-factors are related to the wall surface quality in the region of the leading edge.

Experimental difficulties reduced the Reynolds number range effectively useful for correlation. The flow over the model showed to be too stable up to about $Re_C = 15\times10^6$ to obtain a transition location function of the expected instabilities, and finally the range explored went from about 15 to 23×10^6. Nevertheless, the experiments confirm the possibility to observe laminar-turbulent transition up to $Re_C = 23\times10^6$ in ETW. Experience has been gained on the best running conditions in ETW for large Reynolds number transition experiment, and the TSP imaging system is proved to be an efficient method for transition detection in a wide range of temperatures, from ambient to cryogenic. Finally, N-factor calibration of ETW has been achieved in a rather narrow range of conditions

Concerning transition prediction, it can be stated that:

- The classical envelope method, with a single N-factor, does not produce reliable correlations for this type of configurations. The use of two N-factors, one associated with TS transition and the other with crossflow, appears to be more robust.
- The proposed way of considering incompressible stability theory and computing the crossflow N-factor with the constant β^* strategy for stationary disturbances only could be improved. This approach has a tendency to produce N-factor curves with large values close to the leading edge, decreasing to lower values at transition (so-called pathological cases). Other definitions for N_{CF} could be based on a zero frequency envelope, or using the constant β^* strategy for stationary disturbances in non-local theory. These two definitions have the effect of reducing considerably the number of pathological cases.

As a final comment, a set of test cases will be made available for validation of stability codes, derived from those obtained in the course of this work, with information and datasets allowing cross validation of stability computations in the frame of local and non-local theories.

Acknowledgments

The work presented in this paper was part of the research project TELFONA, performed under contract No. AST4-CT-2005-516109, financed by the European Union. Thanks to Donato de Rosa, who produced the final NOLLY results for CIRA.

References

[1]Collier, F.S., "An Overview of Recent Subsonic Laminar Flow Control Flight Experiments", AIAA Paper 93-2987, 1993

[2]Braslow, A.L., "A History of Suction-type control with Emphasis on Flight Research", Monograph in Aerospace History, No. 13, 1999

[3]Bulgubure, C. and Arnal, D., "Dassault Falcon 50 laminar flow flight demonstrator", First European Forum on Laminar Flow Technology, Hamburg, Germany, March 1992

[4]Schrauf, G., Perraud, J., Vitiello, D. and Lam, F., "Comparison of Boundary Layer Transition Predictions using Flight Test Data" Journal of Aircraft Vol. 35, No. 6, 1998, pp. 891-897, doi: 10.2514/2.2409

[5]Schrauf, G., "Large-scale laminar flow tests evaluated with linear stability theory", AIAA Paper 2001-2444

[6]Smith, A.M.O., and Gamberoni, N., "Transition, pressure gradient and stability theory" - Douglas Aircraft Co, Rept. ES 26388, El Segundo, California (1956)

[7]Van Ingen, J., "A suggested semi-empirical method for the calculation of the boundary layer transition region" - Univ. of Techn., Dept of Aero. Eng., Rept. UTH-74, Delft (1956)

[8]Bartelheimer, W., "Ein Entwurfsverfahren für Tragflügel in transsonischer Strömung, Dissertation TU-Braunschweig, DLR FB 96-30,199.

[9]Schrauf, G., "LILO 2.1 – Users' Guide and Tutorial", GSSC Technical Report, July 2006

[10]Schrauf, G., Horstmann, K. H. and Streit, T., "The Telfona Pathfinder Wing for the Calibration of the ETW Wind Tunnel" Proceedings of the 1st CEAS European Air and Space Conference, 10-13 September, Berlin, 2007.

[11]Fey, U., Egami, Y. and Engler, R. H., "High Reynolds number transition detection by means of Temperature Sensitive Paint", AIAA Paper 2006-0514 (2006).

[12]Schrauf, G., Horstmann, K. H., Streit, T., Perraud, J. and Donelli, R., "The Telfona Pathfinder Wing for the Calibration of the ETW Wind Tunnel" KATnet II Conference on Key Aerodynamic Technologies, 12-14 May, Bremen, 2009

[13]Laburthe, F., "Problème de stabilité linéaire et prévision de la transition dans des configurations tridimensionnelles, incompressibles et compressibles", Thèse de Doctorat Sup'Aéro, Toulouse, Dec. 1992

[14]Malik, M. R., "COSAL – A black-box compressible stability analysis code for transition prediction in three-dimensional boundary layer", NASA CR-165925, 1982.

[15]Perraud, J., Arnal, D., Casalis, G. and Donelli R., "Automatic transition Predictions using Simplified Methods", AIAA Journal, Vol. 47, No. 11, Nov. 2009, pp 2676-2684, doi: 10.2514/1.42990

[16]Hein, S., Bertolotti, F. P., Simen, M., Hanifi, A. and Henningson, D., "Linear non-local instability analysis – the linear NOLOT code –. DLR Internal Report IB 223-94 A56, 1994

[17]Hanifi, A., Henningson, D., Hein, S., Bertolotti, F. P. and Simen, M., "Linear non-local instability analysis – the linear NOLOT code –. FFA TN 1994-54, 1994

[18]De Matteis, P., Donelli, R. and Luchini, R. S., "Application of the ray tracing theory to the stability analysis of three-dimensional incompressible boundary layers", XIII AIDAA Conference, Rome, Italy, 1995